HHS Public Access

Author manuscript

Angew Chem Int Ed Engl. Author manuscript; available in PMC 2024 March 01.

Published in final edited form as:

Angew Chem Int Ed Engl. 2023 March 01; 62(10): e202216309. doi:10.1002/anie.202216309.

Designed Iron Catalysts for Allylic C−H Functionalization of Propylene and Simple Olefins

Ruihan Wang[a,#], **Yidong Wang**[a,#], **Ruiqi Ding**[a], **Parker B. Staub**[a], **Christopher Z. Zhao**[a], **Peng Liu**[a], **Yi-Ming Wang**[a]

[a]Department of Chemistry, University of Pittsburgh, Pittsburgh, Pennsylvania 15260, United States

Abstract

Propylene gas is produced worldwide by steam cracking on million-metric-ton scale per year. It serves as a valuable starting material for π-bond functionalization but is rarely applied in transition metal-catalyzed allylic C−H functionalization for fine chemical synthesis. Herein, we report that a newly-developed cationic cyclopentadienyliron dicarbonyl complex allows for the conversion of propylene to its allylic C−C bond coupling products under catalytic conditions. This approach was also found applicable to the allylic functionalization of simple α-olefins with distinctive branched selectivity. Experimental and computational mechanistic studies supported the allylic deprotonation of the metal-coordinated alkene as the turnover-limiting step and led to insights into the multifaced roles of the newly designed ligand in promoting allylic C−H functionalization with enhanced reactivity and stereoselectivity.

Graphical Abstract

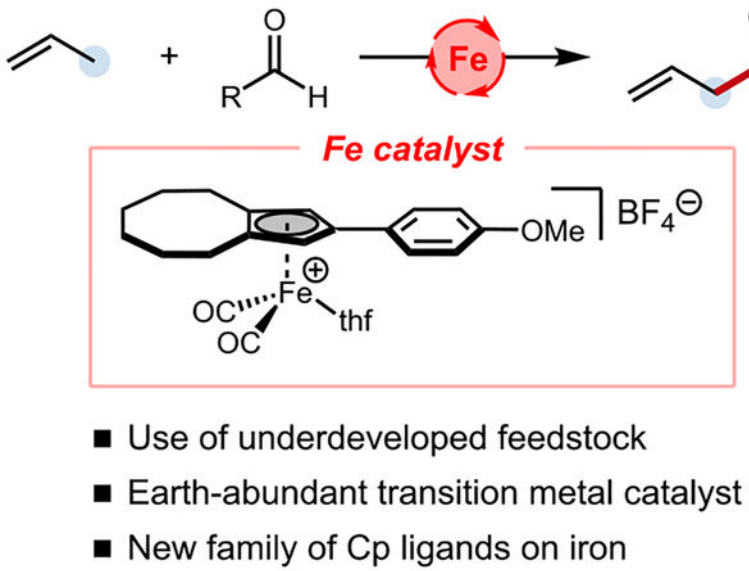

pengliu@pitt.edu, ym.wang@pitt.edu, Twitter accounts: @WangGroupPitt; @pengliu_group.

[#]These authors contributed equally to this work

A new cyclopentadienyliron dicarbonyl complex was discovered to enable the coupling of the allylic carbon of propylene and carbonyl electrophiles. This approach was also successfully applied to allylic C–H functionalization of simple olefins. Experimental and computational studies provided insights into the mechanism and origins of ligand effects on reactivity and diastereoselectivity.

Keywords

iron catalyst; C−H functionalization; propylene; olefin; DFT calculations

Introduction

The production of valuable target molecules from readily available raw materials is a fundamental goal of synthetic chemistry. Transition metal-catalyzed C(sp^3)−H bond activation has become an increasingly powerful tactic for expanding the synthetic toolbox by exploiting simple and abundant chemical building blocks.[1] Propylene, one of the smallest hydrocarbons, is the second largest petrochemical feedstock with an annual global production of over 100 million metric tons.[2] Owing to the versatility of the π-bond, propylene is used to produce a number of commodity chemicals such as polypropylene,[3] isopropyl alcohol, acrylonitrile[4] and propylene oxide.[5] Given the plentiful supply and synthetic utility, propylene has received growing attention in the realm of modern olefin chemistry, with successful employment in a wide array of transformations including hydrofunctionalization,[6] difunctionalization,[7] cycloaddition,[8] ene-type reaction,[9] metathesis[10] and vinylic functionalization.[11]

In contrast to the large number of applications of propylene in π-functionalization reactions, only a handful of synthetic methodologies result in its allylic functionalization. In addition to recently reported stoichiometric functionalization strategies,[12,13] the reactivity of transition metals has enabled the development of more atom economical catalytic processes. In one catalytic approach, the formal allylic functionalization of propylene could be achieved through an initial 1,2-insertion of a metal species into the π-bond of propylene, followed by β-H elimination to generate a transposed C=C bond. This indirect strategy was particularly successful for the Ru-catalyzed synthesis of polyenes reported by Trost.[14a] Applications to base metal catalysis by Ni[9c,d] and Co[14b] have also been reported. However, the control of chemoselectivity of these reactions has proven to be challenging (Scheme 1A, i).

Although conceptually straightforward, the direct C(sp^3)−H functionalization of propylene is underexplored and poorly developed synthetically. While two-electron metalation of alkenes through π-allyl chemistry has emerged as a powerful approach for allylic C−H functionalization,[15] the only example in the context of propylene functionalization was found to proceed in moderate yield, and the substrate scope was not investigated.[16] Recently, the development of radical-mediated allylic functionalization reactions that leverage photoredox and transition metal catalysis has greatly increased the diversity of coupling partners for simple unactivated olefins.[17] However, propylene has stood out as

a particularly challenging substrate for this mode of reactivity, with only a handful of examples proceeding in low or modest yield reported in the literature (Scheme 1A, ii).[18] More recently, Kobayashi described a strong Brønsted base catalyzed imine allylation process using propylene as allyl source.[9a] Though high reactivity was achieved, the applicability of this approach was limited to a class of specialized substrates. Accordingly, the development of broadly applicable methods for C(sp^3)−H functionalization of propylene that deliver a wider range of useful products persists as a largely unmet synthetic challenge.

Our group has been engaged in developing a generic strategy for α-C−H functionalization of π-bonds using cationic iron complexes of type $Cp^XFe(CO)_2^+$ as the catalysts (Cp^X is a substituted cyclopentadienyl ligand; henceforth, $Fp^X = Cp^XFe(CO)_2$).[19] We conceived that this strategy could serve as a platform for the allylic C−H functionalization of propylene. In this approach, the initial metal coordination to a C−C π-bond drastically enhances the acidity of C−H bonds α to the π-bond, allowing for subsequent deprotonation using hindered amine bases. Electrophilic attack of the resulting η^1-iron species with S_E2' selectivity then affords the product of net α-C−H functionalization (Scheme 2a). This catalytic mode has been successfully applied to propargylic and allenylic C−H functionalization, and allylic C−H functionalization at electronically activated sites, delivering a diverse range of products containing new C−C bonds.[19a,c,e–f] By contrast, simple unfunctionalized olefins performed with substantially inferior reactivity, even after further optimization of reaction conditions. In spite of these challenges, we felt that our approach for alkene functionalization possessed several distinct advantages, including 1) use of the most earth-abundant transition metal as catalyst; 2) avoidance of stoichiometric allymetal reagents; and 3) delivery of regiodefined products without concomitant double-bond isomerization.

These advantages prompted us to optimize the iron-catalyzed allylation process. We posited that the inherent lower acidity of allylic C−H bonds (pK_a ~ 43) compared to propargyl C−H bonds (pK_a ~ 35 to 40) contributes to the difficulty of olefin α-functionalization. To address this, we envisaged that altering the substituents on the cyclopentadienyl ligand would modify the electronic and steric environment of the alkene-iron π-complex and could thus accelerate the deprotonation step of the catalytic cycle, which had been proposed to be turnover-limiting in our previously developed catalytic systems.[19e] In addition, we surmised that the tunable ring substituents could be used to modulate stereoselectivity through catalyst-controlled non-covalent interactions in the carbonyl addition transition states.

With these considerations, we were motivated to investigate the application of propylene as a high-utility substrate within the broader context of our ongoing efforts to develop more efficient iron catalysts for allylic C−H functionalization. In this article, we report a mild catalytic addition of allylic C−H bonds of propylene and other simple olefins to carbonyl electrophiles. A new class of cyclopentadienyl ligands for iron catalysts equipped with a cyclooctano ring fusion and electron-rich arene substituents was discovered to enable this transformation. In addition to expanding the utility of propylene as a substrate, these catalysts were also found to improve the diastereoselectivity of reactions using simple α-olefins as substrates, many of which are widely available feedstocks. Stoichiometric

experiments and density functional theory (DFT) calculations were performed to disclose the detailed mechanism of this catalytic system, which also provided insights into the enhanced reactivity and diastereoselectivity promoted by the new catalysts.

Results and Discussion

Identification of a Ligand System for Propylene Functionalization.

In our previously reported allylic functionalization reactions, $[Fp^*(thf)]^+BF_4^-$ was used as the catalyst to enable the coupling of alkenes with commercially available aldehydes.[19f] With this catalyst as a starting point, we initiated the study by examining the reactivity of propylene using 1-naphthaldehyde (**1**) as the model aldehyde coupling partner and one atmospheric pressure of propylene supplied by a balloon (Scheme 3a). This attempt afforded a minimal amount of product. We then conducted the reaction under elevated pressure of propylene using a pressure tube (~8 atm initial pressure, 1.1 mmol of propylene; see SI for details), which resulted in a notable improvement of yield. Though yields were still modest, these preliminary results provided evidence for the possibility of propylene functionalization using our catalytic strategy. Thus, we embarked on a campaign to prepare new ligands and identify structures that would improve catalyst performance.

As an initial hypothesis, we posited that increasing the **π**-acidity of the cationic iron complex would improve catalyst efficiency by facilitating the deprotonation of the iron−alkene complex. Bearing fewer electron-donating alkyl substituents than Cp* and being readily prepared and modifiable, 2-phenyltetrahydroindenyl (Cp^{W1}) was considered as a ligand, and $\mathbf{Fp^{W1}(thf)BF_4}$ was prepared and evaluated as a catalyst (henceforth, $\mathbf{Fp^{X}(thf)BF_4}$ represents $[Fp^X(thf)]^+BF_4^-$) (Scheme 3b).[1a,20] To our delight, this novel catalyst led to higher yield than $\mathbf{Fp^*(thf)BF_4}$. Comparison of the IR stretching frequencies of the CO ligands (ν(CO)) supported our initial intuition of Cp^{W1} being less electron donating. Motivated by the importance of ligand steric effects in our previously developed iron catalysts for allene and alkyne functionalization,[19a,e] we next examined the effect of modifying the fused cyclohexane ring in Cp^{W1}. Indeed, $\mathbf{Fp^{W2}(thf)BF_4}$ bearing a fused cyclooctane ring exhibited still higher efficiency for propylene functionalization. A significantly higher ν(CO) of this complex was also observed, indicating that there may also be a substantial electronic effect from changing the ring size. Fine tuning of the aryl substituents on the cyclopentadienyl ring led to the identification of 4-methoxyphenyl substituted $\mathbf{Fp^{W3}(thf)BF_4}$ as an effective and generally applicable catalyst for the coupling of propylene with aryl aldehydes. The optimized conditions were further refined by additional adjustments of reagent stoichiometries.

A series of control experiments were conducted to rule out the possibility of an ene-type process and supported the indispensable role of iron catalyst in this allylic functionalization process (see SI for details).

Substrate Scope.

With the effective iron catalysts in hand, we evaluated the scope of a variety of aldehydes. Aryl aldehydes with different substitution patterns ranging from highly electron-poor to

mildly electron-rich were all successfully accommodated in our catalytic system (**1a**−**10a**). Among these examples, particular functional groups including an internal alkyne (**3a**), a methyl sulfone (**7a**), an aryl tosylate (**8a**) and a sulfonamide (**9a**) were well tolerated. Moreover, a range of nitrogen-, oxygen- and sulfur-containing heteroaryl aldehydes were examined. We were delighted to find that substrates bearing electron withdrawing groups adjacent to heteroatoms underwent allylation in good yields (**11a**, **15a**−**16a**, **18a**−**19a**). A coumarin-type aldehyde featuring lactone motif was also found to be a suitable coupling partner (**13a**). Electron-rich heteroaryl aldehydes (**12a**, **14a**, **17a**) reacted smoothly, albeit with diminished yields.

Several sterically hindered alkyl aldehydes were subjected to the standard conditions. An acyclic aldehyde derived from gemfibrozil (**20a**) and an aldehyde bearing a cyclic alkyl group (**21a**) reacted efficiently. A piperidine-substituted aldehyde (**22a**) was also a suitable substrate for this reaction. A tetrahydropyran-substituted aldehyde (**23a**) was tolerated well when higher acid and base stoichiometries were employed. Finally, 1,4-benzenedicarbaldehyde underwent diallylation in moderate yield (**24a**) when double amounts of catalyst and reagents were employed.

We further explored the applicability of our protocol by examining substrates incorporated with complex scaffolds of pharmaceutical importance. Aldehydes carrying fenchol (**25a**), probenecid (**26a**), benzbromarone (**27a**) and paroxetine (**29a**) were found to be effective substrates with moderate to good yields. Remarkably, a flufenamic acid-derived aldehyde (**28a**), which contains an unprotected diarylamine, reacted cleanly in our system. During the course of the scope examination, we found that the catalyst loading could be reduced to 5 mol % for highly reactive aldehydes, while the addition of $Zn(NTf_2)_2$ was needed to improve the yield for aldehydes with low reactivity, likely by serving as a Lewis acid that could coordinate to and activate less-reactive aldehydes. In a few cases (**27a**, **28a**), switching the catalyst to $\mathbf{Fp^{W6}(thf)BF_4}$ led to improved yields of the corresponding homoallylic alcohols.

We next investigated the extension of the iron-catalyzed propylene functionalization reaction to other types of electrophiles (Table 2). A pair of *N*-benzylated isatins were selected as coupling partners, which delivered C-3 carbonyl allylation products in good to excellent yields (**30a**, **31a**). We also subjected *N,O*-acetal reagents to the standard conditions, which were previously prepared for allene functionalization by our group.[19a] Pleasingly, propylene reacted efficiently with the *in situ* generated iminium to deliver the desired homoallylic amines (**32a**−**34a**). The use of the diethyl acetals of aryl aldehydes as substrates was also feasible, delivering benzylic ethyl ethers **35a** and **36a** in modest to moderate yields.

Carbonyl Allylation Reactions with Higher Olefins.

After exploring the scope of electrophiles, we wondered whether our methodology could be applied to the allylic C−H functionalization of higher olefins. We commenced the study by subjecting 4-bromobenzaldehyde and 1-octene to our initial conditions (10 mol % $\mathbf{Fp^*(thf)BF_4}$) for catalyst development, which furnished the branched-selective hydroxyalkylation product with modest yield and low level of diastereoselectivity control

(36% yield, 2.0:1 d.r.). Fortunately, we were pleased to find that using the catalyst **$Fp^{W3}(thf)BF_4$** optimized for propylene functionalization led to excellent yield and enhanced diastereoselectivity, even with catalyst loading and reaction temperature reduced to 5 mol % and 45 °C, respectively (see SI for details). An additional improvement of diastereoselectivity was observed by switching the catalyst to **$Fp^{W5}(thf)BF_4$**. Under the modified conditions, several commonly used chlorine-, oxygen- and nitrogen-containing functional groups were tolerated (Table 3), as well as a boronic acid pinacol ester (**5f**) and a thiophene (**5h**). It was also found that the reaction could undergo selective functionalization of allylic C−H bonds in the presence of a propargyl amine (**5i**). X-ray crystallographic analysis of compound **5k** was conducted to confirm the relative configuration of the major diastereomer.[21] We then examined the reactivities of internal olefins. Gratifyingly, several benzocycloalkenes and *cis*-β-methylstyrene could be coupled under the same conditions, notwithstanding the low control of diastereoselectivity (**5p**−**5t**).

Finally, we selected several substrates in each table and examined their reactivities using **Fp*(thf)BF_4** (10 mol %) as the catalyst under the same reaction conditions. The replacement of catalyst generally led to significant decrease in yield, which demonstrates the considerable improvements in catalyst efficiency and functional group tolerance achieved by the newly developed 2nd generation ligand system.

Synthetic Applications.

The propylene functionalization process could be easily scaled up to 3 mmol under a reduced propylene pressure of 2.5 atm. Meanwhile, the allylic functionalization reaction of 1-octene was performed on 10 mmol scale to produce multigram quantities of product **5b** (Scheme 4a). To showcase the versatility of our allylation products, we were interested in using the homoallylic alcohol building blocks to construct some common heterocycle motifs. Three of the products (**4a**, **12a**, **15a**) were derivatized into molecules containing lactone- (**37**), tetrahydropyran- (**38**) and dihydropyrazole (**39**) moieties through multistep transformations (Scheme 4b). Moreover, we demonstrated the manipulation of the C=C bond by applying modern CuH catalysis,[22] leading to an anti-Markovnikov hydroamination product (**40**).

Mechanistic Studies.

In order to understand the superior reactivity of **$Fp^{W3}(thf)BF_4$** catalyst and the overall mechanism, we performed kinetic studies and stoichiometric reactions of the deprotonation step. We began our investigation by examining the kinetic isotope effect using 1-decene (**u**) and its allylic-deuterated isotopologue (**u-*d_2***). Initial rate experiments conducted in parallel yielded a k_H/k_D of 2.8, and an intermolecular competition experiment resulted in the same KIE value (Scheme 5a). The primary kinetic isotope effect measured in both sets of experiments suggests that proton abstraction is likely the turnover-limiting step.

On that basis, we suspected that the different performances between catalysts based on Fp^{W3} and Fp* mainly result from the differences of their abilities to promote the deprotonation step. A series of cationic Fp^X-alkene (Fp^X = Fp* or Fp^{W3}) complexes (**Int-1**) were prepared by adding the alkene to a solution of $Fp^X(thf)BF_4$ for the comparison of their stoichiometric

reactivities. Deprotonation reactions were performed by treating these complexes with Et_3N in CD_2Cl_2 for 2 h, by which time no further conversion could be detected. Although the equilibrium constants for deprotonation could not be determined due to the formation of side products, we were able to determine the NMR yields of the deprotonation products (Scheme 5b) as well as other quantifiable species in each reaction mixture (see SI for details). In line with our hypothesis, the deprotonation yields of all Fp^{W3}-alkene complexes were significantly higher than those of Fp*-alkene complexes, indicating a more facile cleavage of the allylic C−H bonds enabled by Fp^{W3}. During the course of deprotonation of Fp*-alkene complexes, we observed significant amounts of free alkenes especially in the case of 1-hexene, suggesting that dissociation of the substrate is a competitive process. In contrast, this behavior was not observed for Fp^{W3}-alkene complexes. Thus, from the view of the stoichiometric deprotonation step, the new catalyst **Fp^{W3}(thf)BF_4** enhances the desired reactivity of the Fp^X-alkene species while inhibiting the tendency for the alkene to dissociate.

To provide additional evidence for our proposed catalytic cycle, we conducted the electrophilic functionalization reactions of Fp* and Fp^{W3}-based allyliron species **II-v** (Scheme 5c). Although compounds **II-v** could not be purified, the desired allylic functionalization product **5v** can be obtained by treating the cationic complexes **I-v** with Et_3N for 2 h to effect deprotonation, and subsequently subjecting the crude mixture to the solution of 4-bromobenzaldehyde (**5**) and BF_3•Et_2O. Consistent with catalytic results, the Fp^{W3}-based complex delivered a significantly higher yield of the coupling product **5v** compared to the Fp*-based complex.

Computational Studies.

Density functional theory (DFT) calculations were carried out to explore the mechanistic details regarding the origins of diastereoselectivity and ligand effects on catalyst reactivity. We calculated the reaction energy profile of the coupling of 1-butene and benzaldehyde using an Fp^{W3}-based catalyst (see Table S1 for computational results with other substrates). The calculations were performed at the M06/6–311+G(d,p)−SDD(Fe)/SMD(toluene)//B3LYP-D3(BJ)/6–31G(d)−SDD(Fe) level of theory and conformational sampling was conducted with CREST/GFN2-xTB[23] (see SI for computational details). Starting from the cationic Fp^{W3}-alkene complex **41**, the coordination of its allylic C–H bond to TMPH generates hydrogen-bonding complex **42**, which then undergoes C–H deprotonation–metalation via **TS1** to deliver allyliron species **43**.[24] Because the 18-electron complex **41** is coordinatively saturated, the deprotonation involves an external base,[25] cleaving the *anti* C–H bond with respect to the iron center (**TS1**).[26] The subsequent electrophilic addition of the aldehyde to the coordinatively saturated allyliron species **43** takes place via open transition states **TS2** and **TS2'** and determines the diastereoselectivity of this reaction. While high levels of diastereoselectivities are often achieved in the addition of allylmetal species to aldehydes through closed Zimmerman−Traxler-type transition states,[27] catalyst control of diastereoselectivity through open transition states is often challenging due to the lack of direct interactions between the catalyst and the carbonyl moiety.[28] In this reaction, our calculations indicate that the addition of a BF_3-coordinated benzaldehyde (**46)** to **43** favors the (*R**,*S**) diastereomer **44** (*via* **TS2**) over the (*R*,R**) diastereomer **44'** (*via*

TS2') by 0.3 kcal/mol (see Figure S1 in SI for other higher energy TS conformers).[29] Although the computed activation free energy difference ($\Delta\Delta G^{\ddagger}$) slightly underestimates the diastereoselectivity (experimental *d.r.* of 4.8:1 versus computationally predicted *d.r.* of 1.6:1), computations predicted the same major diastereomer as that observed experimentally. A better agreement with experimental *d.r.* was obtained at the DLPNO-CCSD(T)[30]/def2-TZVP/SMD(toluene) level of theory (Figure 1b, $\Delta\Delta G^{\ddagger}$ = 0.9 kcal/mol, corresponding to a predicted *d.r.* of 4.2:1. See Table S1 in the SI for detailed benchmark studies using DLPNO-CCSD(T) and other DFT methods).

Next, we analyzed factors that affect the diastereoselectivity-determining aldehyde addition transition states. In both **TS2** and **TS2'**, the phenyl group on the aldehyde is located proximal to the aryl substituent on the Cp^{W3} ligand. These geometries are stabilized by **π**/**π** interactions between the Cp^{W3} ligand and benzaldehyde (see Figures S2 and S3 in SI. Higher energy TS conformers lack the stable **π**/**π** interaction between ligand and substrate). Transition state **TS2**, where the allyliron species attacks the (*Si*)-face of the BF_3-coordinated aldehyde, exhibits a synclinal disposition of the C=C bond relative to the carbonyl group. On the other hand, **TS2'**, which allows (*Re*)-face attack, is an antiperiplanar transition state. Although the synclinal conformation of **TS2** suffers from a slightly greater steric repulsion, this is compensated by two favorable C–H···F hydrogen bonds (*d* = 2.10 and 2.29 Å, respectively) between the two partial positively charged C–H bonds on the allyl moiety and one partial negatively charged F atom on the BF_3•aldehyde complex.[31] However, in **TS2'**, where the aldehyde carbon is antiperiplanar with the C=C bond, only one weaker C–H···F hydrogen bond (*d* = 2.38 Å) was observed because the BF_3 group on the aldehyde carbonyl is pointing away from the allyl moiety. **TS2** is also stabilized by stronger **π**/**π** interactions between the Cp^{W3} ligand and benzaldehyde, as evidenced by the shorter distance between the two benzene rings in **TS2** (4.27 Å) compared to that in **TS2'** (4.68 Å). Taken together, the DFT calculations revealed that the stereochemical control in the open transition states is due to the **π**/**π** interaction with the aryl substituent on the Cp^{W3} ligand anchoring the orientation of the aldehyde, whereas the **π**-facial selectivity of the aldehyde is determined by the C–H···F hydrogen bonding interactions that promotes a synclinal conformation leading to the preferred (*R**,*S**) diastereomeric product.

The overall reaction energy profile shown in Figure 1a suggests that the C–H deprotonation by TMPH is the turnover-limiting step of the catalytic cycle. This is consistent with the primary KIE observed experimentally (Scheme 5a). Next, we examined the ligand effect on reactivity by comparing the computed C–H deprotonation barriers using catalysts based on Fp^{W3} and Fp* (Figure 1c, computed in CH_2Cl_2 to consist with experimental condition in Scheme 5b). The DFT calculations indicate that the Fp^{W3}-based catalyst promotes the C–H deprotonation both kinetically and thermodynamically. Compared to the Fp*-alkene complex, the deprotonation of Fp^{W3}-alkene complex is less endergonic by 1.4 kcal/mol and requires a 1.7 kcal/mol lower barrier. The deprotonation transition state with the Cp^{W3} ligand (**TS1**) is stabilized by a C–H/**π** interaction between a methyl substituent on TMPH and the electron-rich *p*-$MeOC_6H_4$ group on the Cp^{W3} ligand (Figure 1c). In addition, with the sterically less hindered Cp^{W3} ligand, steric repulsion between the Cp ligand and the allyl

group is diminished, as evidenced by the longer H···H distance between the ligand and the allylic C–H in **TS1** (2.44 Å) than in **TS3** (2.19 Å).

Conclusion

We have described a new strategy for the direct functionalization of the allylic C(sp^3)–H bonds of propylene, an abundant C3 hydrocarbon building block, by employing a newly-developed family of cationic iron dicarbonyl complexes as the catalysts. This protocol was also applicable for the allylic functionalization of a range of simple α-olefins. Mechanistic studies based on experiments and DFT calculations provided an understanding of the overall energetic profile of the reaction and insights into the ligand enabled improvements in efficiency and stereoselectivity. Additional applications of ligand design to α-functionalization of π-bonds are ongoing in our laboratories.

Supplementary Material

Refer to Web version on PubMed Central for supplementary material.

Acknowledgements

We acknowledge the ACS PRF (61422-DNI1 for Y.-M.W.), the National Institutes of Health (R35GM142945 for Y.-M.W. R35GM128779 for P.L.), and start-up funding from the University of Pittsburgh (Y.-M.W.). DFT calculations were performed at the Center for Research Computing of the University of Pittsburgh and the Extreme Science and Engineering Discovery Environment (XSEDE). We are very thankful to Dr. Xiao-Dong Zuo for initial investigations into the reactivity of some iron complexes and his mentorship on students continuing the discovery of new catalysts.

References

[1]. Selected reviews for C−H activation:(a)Jardim GAM, de Carvalho RL, Nunes MP, Machado LA, Almeida LD, Bahou KA, Bower JF, da Silva EN Junior, Chem. Commun 2022, 58, 3101–3121. (b)Pulcinella A, Mazzarella D, Noel T, Chem. Commun 2021, 57, 9956–9967.(c)Gandeepan P, Muller T, Zell D, Cera G, Warratz S, Ackermann L, Chem. Rev 2019, 119, 2192–2452. [PubMed: 30480438] (d)Chen Z, Rong MY, Nie J, Zhu XF, Shi BF, Ma JA, Chem. Soc. Rev 2019, 48, 4921–4942. [PubMed: 31403147] (e)Saint-Denis TG, Zhu RY, Chen G, Wu QF, Yu JQ, Science 2018, 359, eaao4798.

[2]. Amghizar I, Vandewalle LA, Van Geem KM, Marin GB, Engineering 2017, 3, 171–178.

[3]. (a)Nifant'ev IE, Ivchenko PV, Bagrov VV, Okumura Y, Elder M, Churakov AV, Organometallics 2011, 30, 5744–5752.(b)Gornshtein F, Kapon M, Botoshansky M, Eisen MS, Organometallics 2007, 26, 497–507.

[4]. Brazdil JF, Appl. Catal., A 2017, 543, 225–233.

[5]. Huang J, Haruta M, Res. Chem. Intermed 2011, 38, 1–24.

[6]. Selected reports:(a)Quach L, Dutta S, Pflüger PM, Sandfort F, Bellotti P, Glorius F, ACS Catal. 2022, 12, 2499–2504.(b)Yang ZP, Fu GC, J. Am. Chem. Soc 2020, 142, 5870–5875. [PubMed: 32176494] (c)Vogt DB, Seath CP, Wang H, Jui NT, J. Am. Chem. Soc 2019, 141, 13203–13211. [PubMed: 31369264] (d)Xing D, Qi X, Marchant D, Liu P, Dong G, Angew. Chem. Int. Engl 2019, 58, 4366–4370.(e)Azpíroz R, Di Giuseppe A, Passarelli V, Pérez-Torrente JJ, Oro LA, Castarlenas R, Organometallics 2018, 37, 1695–1707.(f)Xing D, Dong G, J. Am. Chem. Soc 2017, 139, 13664–13667. [PubMed: 28918637] (g)Li H, Dong K, Jiao H, Neumann H, Jackstell R, Beller M, Nat. Chem 2016, 8, 1159–1166. [PubMed: 27874861] (h)Crisenza GE, Sokolova OO, Bower JF, Angew. Chem. Int. Ed 2015, 54, 14866–14870.(i)Sevov CS, Zhou JS, Hartwig JF, J. Am. Chem. Soc 2014, 136, 3200–3207. [PubMed: 24483848] (j)Sevov CS, Hartwig JF, J.

Am. Chem. Soc 2013, 135, 9303–9306. [PubMed: 23758128] (k)Yamaguchi E, Mowat J, Luong T, Krische MJ, Angew. Chem. Int. Ed 2013, 52, 8428–8431.

[7]. Selected reports:(a)Wang H, Bellotti P, Zhang X, Paulisch TO, Glorius F, Chem 2021, 7, 3412–3424.(b)Li Y, Wei H, Wu D, Li Z, Wang W, Yin G, ACS Catal. 2020, 10, 4888–4894.(c)Li L, Gong T, Lu X, Xiao B, Fu Y, Nat. Commun 2017, 8, 345. [PubMed: 28839152] (d)Mlynarski SN, Schuster CH, Morken JP, Nature 2014, 505, 386–390. [PubMed: 24352229]

[8]. Selected reports:(a)Paulisch TO, Mai LA, Strieth-Kalthoff F, James MJ, Henkel C, Guldi DM, Glorius F, Angew. Chem. Int. Ed 2022, 61, e2021126.(b)Holst DE, Wang DJ, Kim MJ, Guzei IA, Wickens ZK, Nature 2021, 596, 74–79. [PubMed: 34157720] (c)Ma J, Chen S, Bellotti P, Guo R, Schäfer F, Heusler A, Zhang X, Daniliuc C, Brown MK, Houk KN, Glorius F, Science 2021, 371, 1338–1345. [PubMed: 33766881] (d)Kennedy CR, Joannou MV, Steves JE, Hoyt JM, Kovel CB, Chirik PJ, ACS Catal. 2021, 11, 1368–1379. [PubMed: 34336370] (e)Kennedy CR, Zhong H, Joannou MV, Chirik PJ, Adv. Synth. Catal 2020, 362, 404–416. [PubMed: 32431586] (f)Montesinos-Magraner M, Costantini M, Ramirez-Contreras R, Muratore ME, Johansson MJ, Mendoza A, Angew. Chem. Int. Ed 2019, 58, 5930–5935.(g)Lv J, Zhang L, Luo S, Cheng JP, Angew. Chem. Int. Ed 2013, 52, 9786–9790.

[9]. (a)Yamashita Y, Sato I, Fukuyama R, Kobayashi S, Chem. Commun 2022, 58, 2866–2869. (b)Markovic D, Volla CM, Vogel P, Varela-Alvarez A, Sordo JA, Chem. Eur. J 2010, 16, 5969–5975. [PubMed: 20397251] (c)Ho C-Y, Ng S-S, Jamison TF, J. Am. Chem. Soc 2006, 128, 5362–5363. [PubMed: 16620106] (d)Ng S-S, Ho C-Y, Jamison TF, J. Am. Chem. Soc 2006, 128, 11513–11528. [PubMed: 16939275]

[10]. (a)Kalbarczyk KP, Diver ST, J. Org. Chem 2009, 74, 2193–2196. [PubMed: 19203219] (b)Raju R, Allen LJ, Le T, Taylor CD, Howell AR, Org. Lett 2007, 9, 1699–1701. [PubMed: 17407303] (c)Giessert AJ, Diver ST, J. Org. Chem 2005, 70, 1046–1049. [PubMed: 15675867]

[11]. Selected reports:(a)Dong J, Yuan XA, Yan Z, Mu L, Ma J, Zhu C, Xie J, Nat. Chem 2021, 13, 182–190. [PubMed: 33318674] (b)Herbort JH, Lalisse RF, Hadad CM, RajanBabu TV, ACS Catal. 2021, 11, 9605–9617. [PubMed: 34745711] (c)Wang Z, Jiang L, Sarro P, Suero MG, J. Am. Chem. Soc 2019, 141, 15509–15514. [PubMed: 31514502] (d)Casnati A, Gemoets HPL, Motti E, Della Ca N, Noel T, Chem. Eur. J 2018, 24, 14079–14083. [PubMed: 30079970] (e)Schmidt VA, Kennedy CR, Bezdek MJ, Chirik PJ, J. Am. Chem. Soc 2018, 140, 3443–3453. [PubMed: 29414238] (f)Sevov CS, Hartwig JF, J. Am. Chem. Soc 2014, 136, 10625–10631. [PubMed: 25032781] (g)Lee D-H, Kwon K-H, Yi CS, Science 2011, 333, 1613–1616. [PubMed: 21921195] (h)Matsubara R, Jamison TF, J. Am. Chem. Soc 2010, 132, 6880–6881. [PubMed: 20433144]

[12]. Wang DJ, Targos K, Wickens ZK, J. Am. Chem. Soc 2021, 143, 21503–21510. [PubMed: 34914394]

[13]. Qin L, Sharique M, Tambar UK, J. Am. Chem. Soc 2019, 141, 17305–17313. [PubMed: 31613609]

[14]. (a)Trost BM, Gholami H, J. Am. Chem. Soc 2018, 140, 11623–11626. [PubMed: 30173519] (b)Atienza CC, Diao T, Weller KJ, Nye SA, Lewis KM, Delis JG, Boyer JL, Roy AK, Chirik PJ, J. Am. Chem. Soc 2014, 136, 12108–12118. [PubMed: 25068530] For the reaction of propylene with gold-stabilized carbocations, see:(c)Barluenga J, Lonzi G, Tomas M, Lopez LA, Chem. Eur. J 2013, 19, 1573–1576. [PubMed: 23255306]

[15]. Selected reviews:(a)Muzart J, Adv. Synth. Catal 2022, 364, 2268–2288.(b)Kazerouni AM, McKoy QA, Blakey SB, Chem. Commun 2020, 56, 13287–13300.(c)Manoharan R, Jeganmohan M, Eur. J. Org. Chem 2020, 2020, 7304–7319.(d)Wang P-S, Gong L-Z, Acc. Chem. Res 2020, 53, 2841–2854. [PubMed: 33006283] (e)Fernandes RA, Nallasivam JL, Org. Biomol. Chem 2019, 17, 8647–8672. [PubMed: 31553038] (f)Bayeh L, Tambar UK, ACS Catal. 2017, 7, 8533–8543. [PubMed: 30009088] (g)Liron F, Oble J, Lorion MM, Poli G, Eur. J. Org. Chem 2014, 2014, 5863–5883.(h)White M, Synlett 2012, 23, 2746–2748.Selected reports on carbonyl allylation with α-olefins:(i)Deng HP, Eriksson L, Szabo KJ, Chem. Commun 2014, 50, 92076–9210.(j)Tao ZL, Li XH, Han ZY, Gong LZ, J. Am. Chem. Soc 2015, 137, 4054–4057. [PubMed: 25754467] (k)Li LL, Tao ZL, Han ZY, Gong LZ, Org. Lett 2017, 19, 102–105. [PubMed: 27997211]

[16]. Fan LF, Wang PS, Gong LZ, Org. Lett 2019, 21, 6720–6725. [PubMed: 31403315]

[17]. Selected reviews:(a)Yue H, Zhu C, Huang L, Dewanji A, Rueping M, Chem. Commun 2021, 58, 171–184.(b)Huang HM, Bellotti P, Glorius F, Chem. Soc. Rev 2020, 49, 6186–6197. [PubMed: 32756671] (c)Han JF, Guo P, Zhang XG, Liao JB, Ye KY, Org. Biomol. Chem 2020, 18, 7740–7750. [PubMed: 32940308] Selected reports on radical-mediated carbonyl allylation through C−H functionalization:(d)Schwarz JL, Schafers F, Tlahuext-Aca A, Luckemeier L, Glorius F, J. Am. Chem. Soc 2018, 140, 12705–12709. [PubMed: 30216059] (e)Mitsunuma H, Tanabe S, Fuse H, Ohkubo K, Kanai M, Chem. Sci 2019, 10, 3459–3465. [PubMed: 30996935]

[18]. (a)Tanabe S, Mitsunuma H, Kanai M, J. Am. Chem. Soc 2020, 142, 12374–12381. [PubMed: 32605370] (b)Xie W, Heo J, Kim D, Chang S, J. Am. Chem. Soc 2020, 142, 7487–7496. [PubMed: 32233362]

[19]. (a)Wang Y, Scrivener SG, Zuo XD, Wang R, Palermo PN, Murphy E, Durham AC, Wang YM, J. Am. Chem. Soc 2021, 143, 14998–15004. [PubMed: 34491051] (b)Zhu J, Durham AC, Wang Y, Corcoran JC, Zuo X-D, Geib SJ, Wang Y-M, Organometallics 2021, 40, 2295–2304.(c)Xia Y, Wade NW, Palermo PN, Wang Y, Wang YM, Chem. Commun 2021, 57, 13329–13332.(d)Wang Y-M, Durham AC, Wang Y, Synlett 2020, 31, 1747–1752.(e)Wang Y, Zhu J, Guo R, Lindberg H, Wang YM, Chem. Sci 2020, 11, 12316–12322. [PubMed: 34094439] (f)Wang Y, Zhu J, Durham AC, Lindberg H, Wang Y-M, J. Am. Chem. Soc 2019, 141, 19594–19599. [PubMed: 31791121] For overview on iron catalysis, see:(g)Guethmundsson A, Backvall JE, Molecules 2020, 25, 1349. [PubMed: 32188092] (h)Gaillard S, Renaud JL, ChemSusChem 2008, 1, 505–509. [PubMed: 18702146]

[20]. Selected reviews:(a)Piou T, Rovis T, Acc. Chem. Res 2018, 51, 170–180. [PubMed: 29272106] (b)Piou T, Romanov-Michailidis F, Romanova-Michaelides M, Jackson KE, Semakul N, Taggart TD, Newell BS, Rithner CD, Paton RS, Rovis T, J. Am. Chem. Soc 2017, 139, 1296–1310. [PubMed: 28060499] (c)Trost BM, Ryan MC, Angew. Chem. Int. Ed 2017, 56, 2862–2879. (d)Quintard A, Rodriguez J, Angew. Chem. Int. Ed 2014, 53, 4044–4055.Selected reports on substituted tetrahydroindenyl ligands:(e)Asachenko AF, Bush AA, Smirnov AY, Morozov OS, Dzhevakov PB, Kim SY, Cho MS, Lee KS, Lee YH, Cho KJ, Lee SM, Nechaev MS, Russ. Chem. Bull 2016, 65, 1580–1585.(f)Zhou S, Fleischer S, Junge K, Beller M, Angew. Chem. Int. Ed 2011, 50, 5120–5124.(g)Polo E, Barbieri A, Traverso O, Eur. J. Inorg. Chem 2003, 2003, 324–330.(h)Dreier T, Hannig F, Erker G, Bergander K, Fröhlich R, J. Phys. Org. Chem 2002, 15, 582–589.(i)Knölker H-J, Baum E, Goesmann H, Klauss R, Angew. Chem. Int. Ed 1999, 38, 2064–2066.(j)Polo E, Bellabarba RM, Prini G, Traverso O, Green MLH, J. Organomet. Chem 1999, 577, 211–218.(k)Halterman RL, Ramsey TM, J. Organomet. Chem 1994, 465, 175–179.

[21]. Deposit number: CCDC 2207631.

[22]. Zhu S, Buchwald SL, J. Am. Chem. Soc 2014, 136, 15913–15916. [PubMed: 25339089]

[23]. Pracht P, Bohle F, Grimme S, Phys. Chem. Chem. Phys 2020, 22, 7169–7192. [PubMed: 32073075]

[24]. The C–H deprotonation to form the *Z*-stereoisomer of the allyliron species requires a 0.3 kcal/mol higher barrier than **TS1**. See SI, Figure S1, for details.

[25]. (a)Li T, Cheng X, Qian P, Zhang L, Nat. Catal 2021, 4, 164–171. [PubMed: 34755042] (b)Wu B, Su HZ, Wang ZY, Yu ZD, Sun HL, Yang F, Dou JH, Zhu R, J. Am. Chem. Soc 2022, 144, 4315–4320. [PubMed: 35245047] (c)Zheng L, Yan Z, Ren Q, Appl. Organomet. Chem 2022, 36, e6549.(d)Zhong K, Shan C, Zhu L, Liu S, Zhang T, Liu F, Shen B, Lan Y, Bai R, J. Am. Chem. Soc 2019, 141, 5772–5780. [PubMed: 30887803]

[26]. Our DFT calculations indicate that dissociation of BF_3•TMPH adduct to TMPH (the external base) and BF_3 is endergonic by 8.9 kcal/mol, whereas the binding of BF_3 with benzaldehyde is exergonic by −1.8 kcal/mol.

[27]. Dong Y, Schuppe AW, Mai BK, Liu P, Buchwald SL, J. Am. Chem. Soc 2022, 144, 5985–5995. [PubMed: 35341240] (b)Bai DC, Yu FL, Wang WY, Chen D, Li H, Liu QR, Ding CH, Chen B, Hou XL, Nat. Commun 2016, 7, 11806. [PubMed: 27283477] (c)Mahrwald R, Chem. Rev 1999, 99, 1095–1120. [PubMed: 11749441]

[28]. Jiang S, Agoston GE, Chen T, Cabal MP, Turos E, Organometallics 1995, 14, 4697–4709. (b)Denmark SE, Weber EJ, J. Am. Chem. Soc 1984, 106, 7971–7973.(c)Hayashi T, Kabeta K, Hamachi I, Kumad M, Tetrahedron Lett. 1983, 24, 2865–2868.(d)Keck GE, Abbott DE, Boden

EP, Ehnolm EJ, Tetrahedron Lett. 1984, 25, 3927–3930.(e)Li T, Zhang L, J. Am. Chem. Soc 2018, 140, 17439–17443. [PubMed: 30525525]

[29]. The allylation of **43** and its *Z*-isomer were separately analyzed, and both were computed to favor formation of the (*R**,*S**) diastereomer **44** over (*R**,*R**) diastereomer **44'**. See SI for details.

[30]. Guo Y, Riplinger C, Becker U, Liakos DG, Minenkov Y, Cavallo L, Neese F, J. Chem. Phys 2018, 148, 011101. [PubMed: 29306283]

[31]. Thomas AA, Speck K, Kevlishvili I, Lu Z, Liu P, Buchwald SL, J. Am. Chem. Soc 2018, 140, 13976–13984. [PubMed: 30244567]

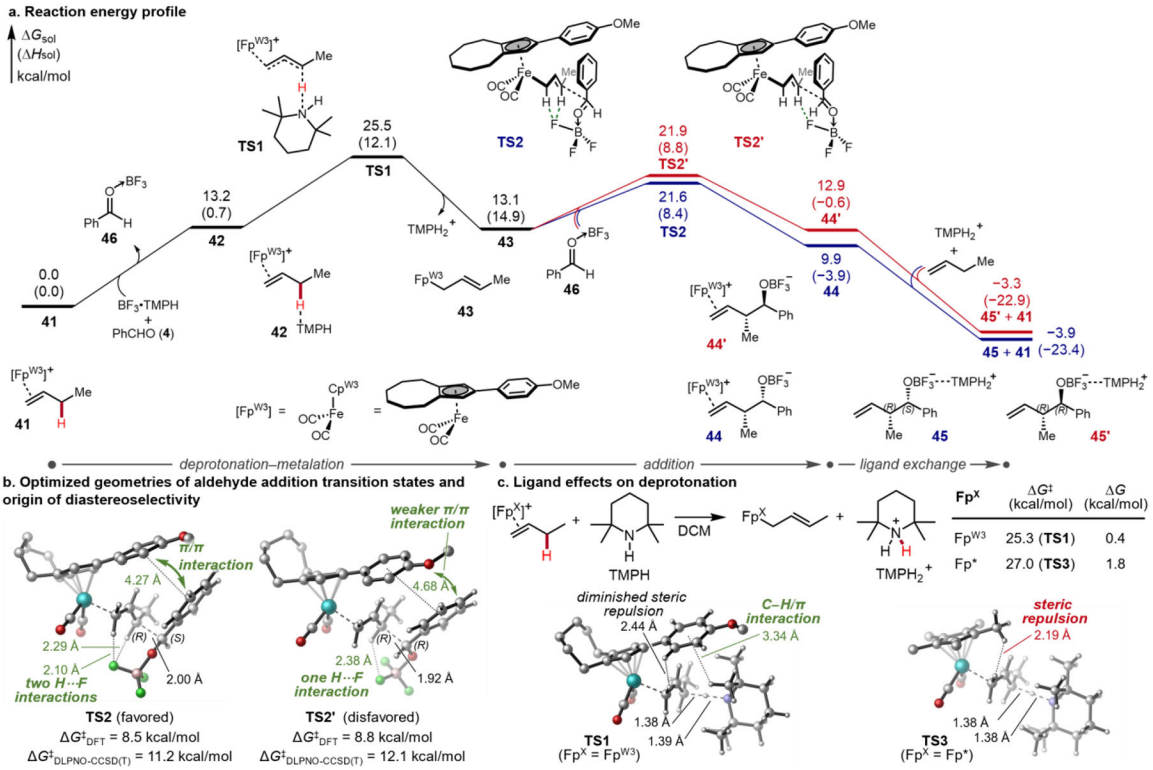

Figure 1.
Computational studies.

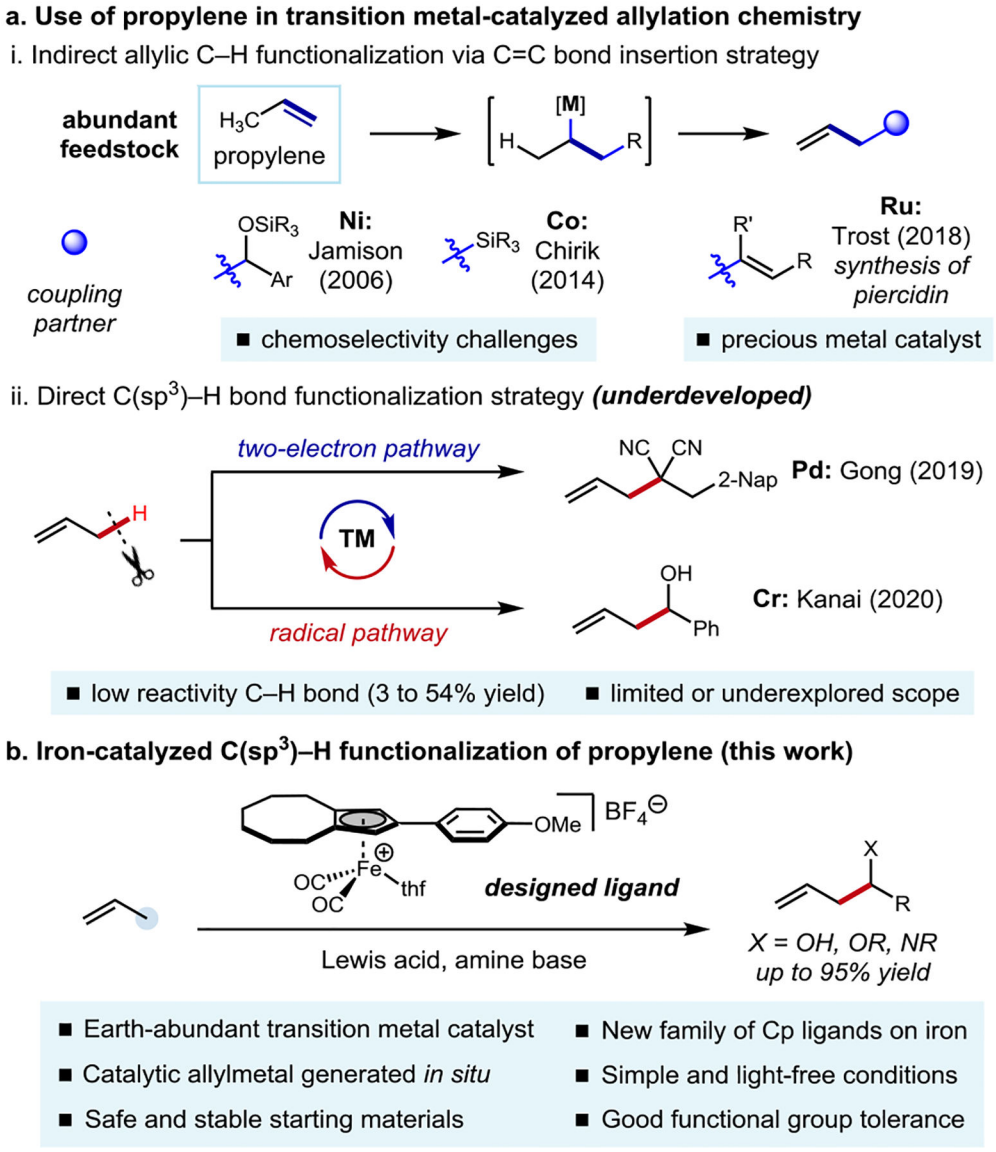

Scheme 1.

Application of propylene as a reagent for allylic functionalization.

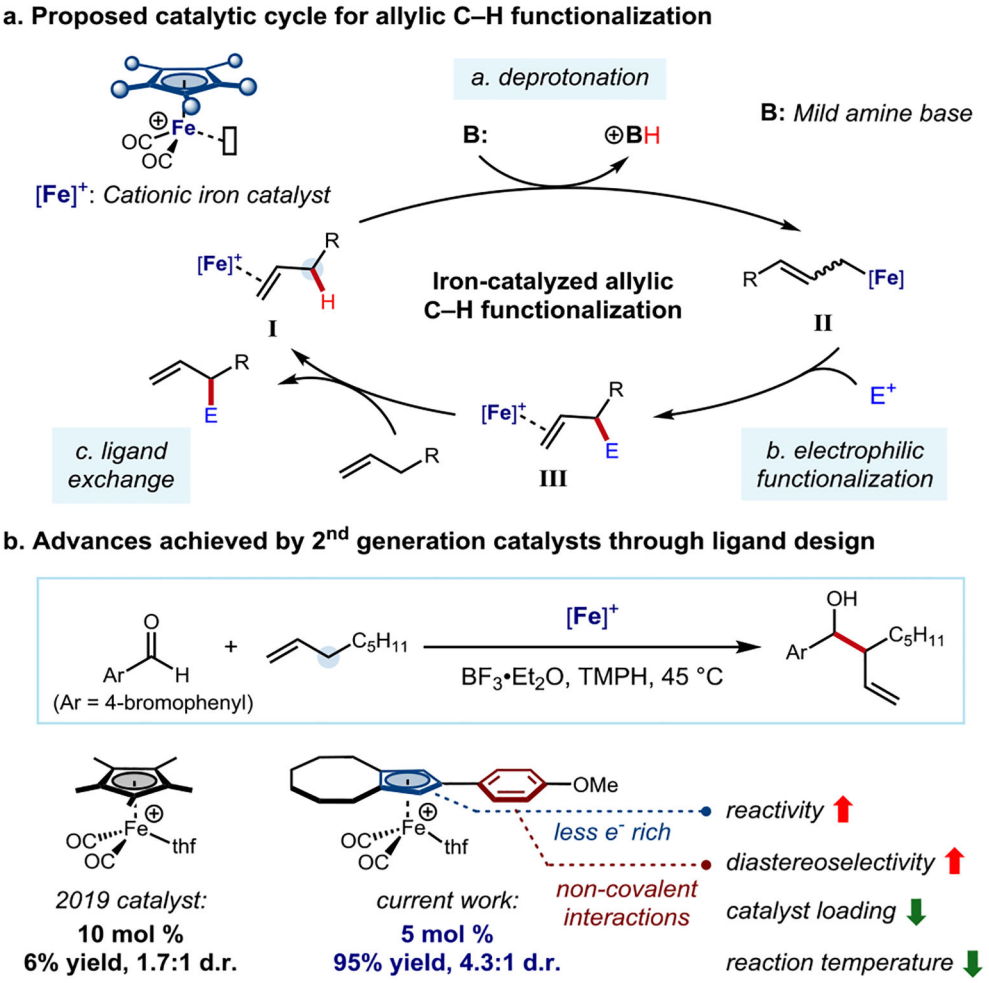

Scheme 2.

Synopsis of ligand design approach for the iron-catalyzed allylic C−H functionalization.

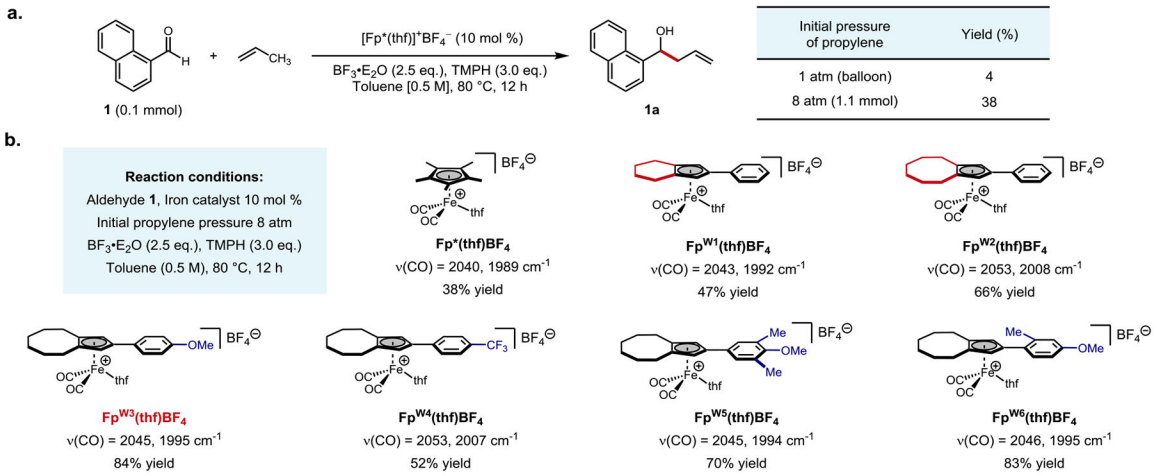

Scheme 3.

Development of iron-catalyzed allylic C−H functionalization of propylene. **a**, Initial results obtained by using $[Fp^*(thf)]^+BF_4^-$ as the catalyst. Yields were determined by ^1H NMR using 2,4-dinitrotoluene as the internal standard. **b**, Examination of catalyst reactivity on the reaction in **a**. Yields were determined by ^1H NMR using 2,4-dinitrotoluene as the internal standard (0.1 mmol scale).

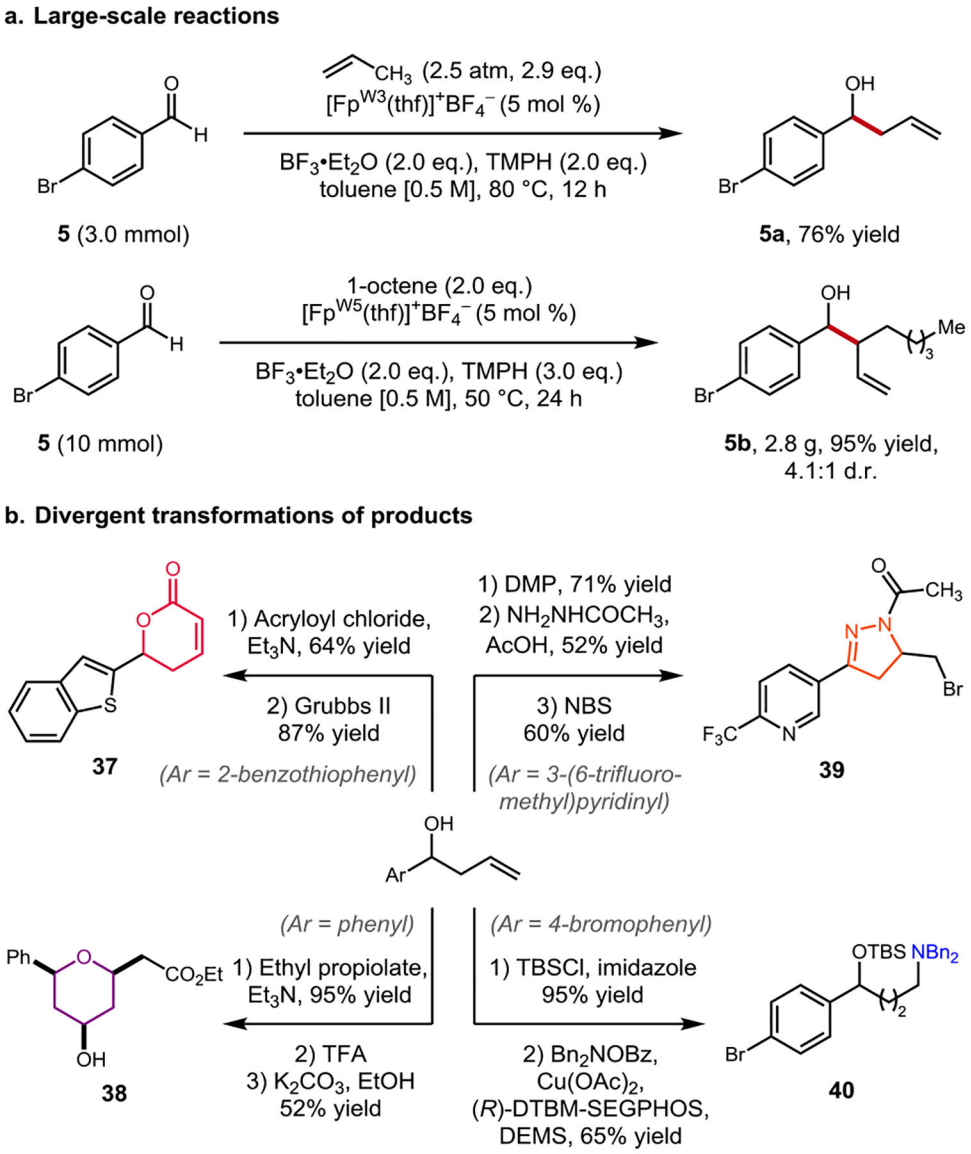

Scheme 4.
Synthetic applications.

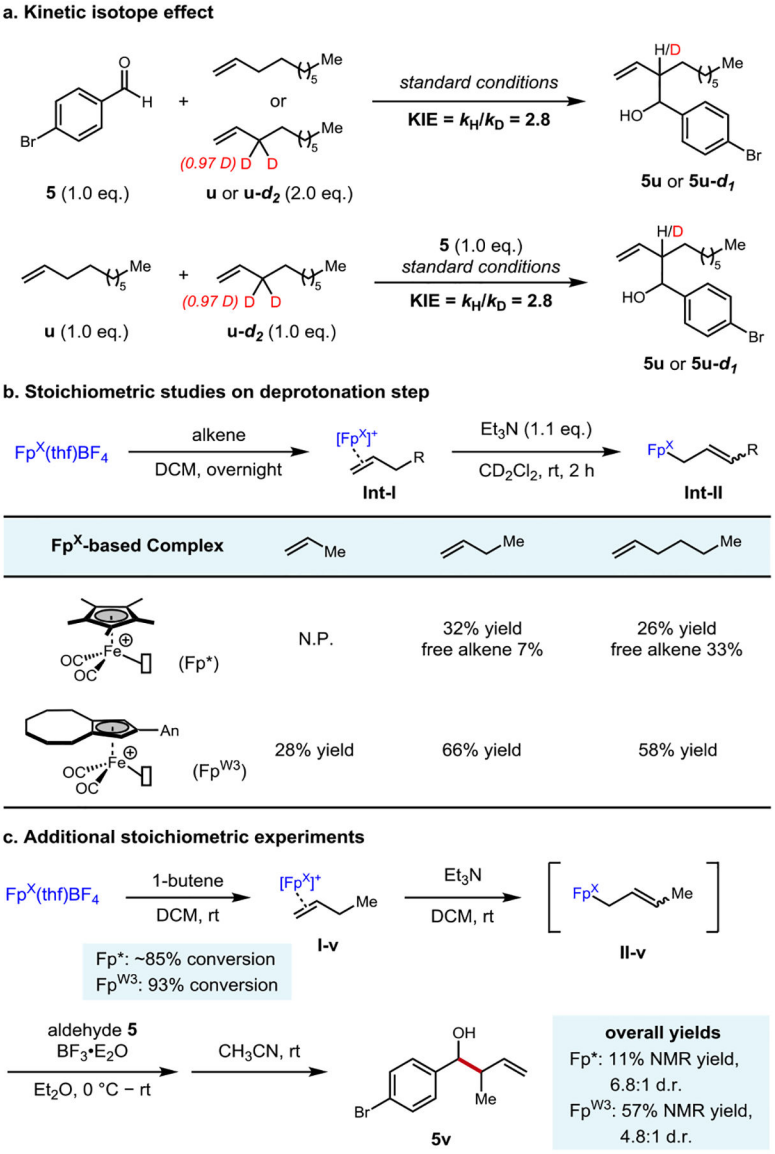

Scheme 5.

Mechanistic experiments. Standard conditions: $[Fp^{W5}(thf)]^{+}BF_4^{-}$ (5 mol %), $BF_3{\bullet}Et_2O$ (2.0 eq.), TMPH (3.0 eq.), toluene (0.5 M), 45 °C.

Table 1.

Aldehyde scope for the functionalization of propylene.

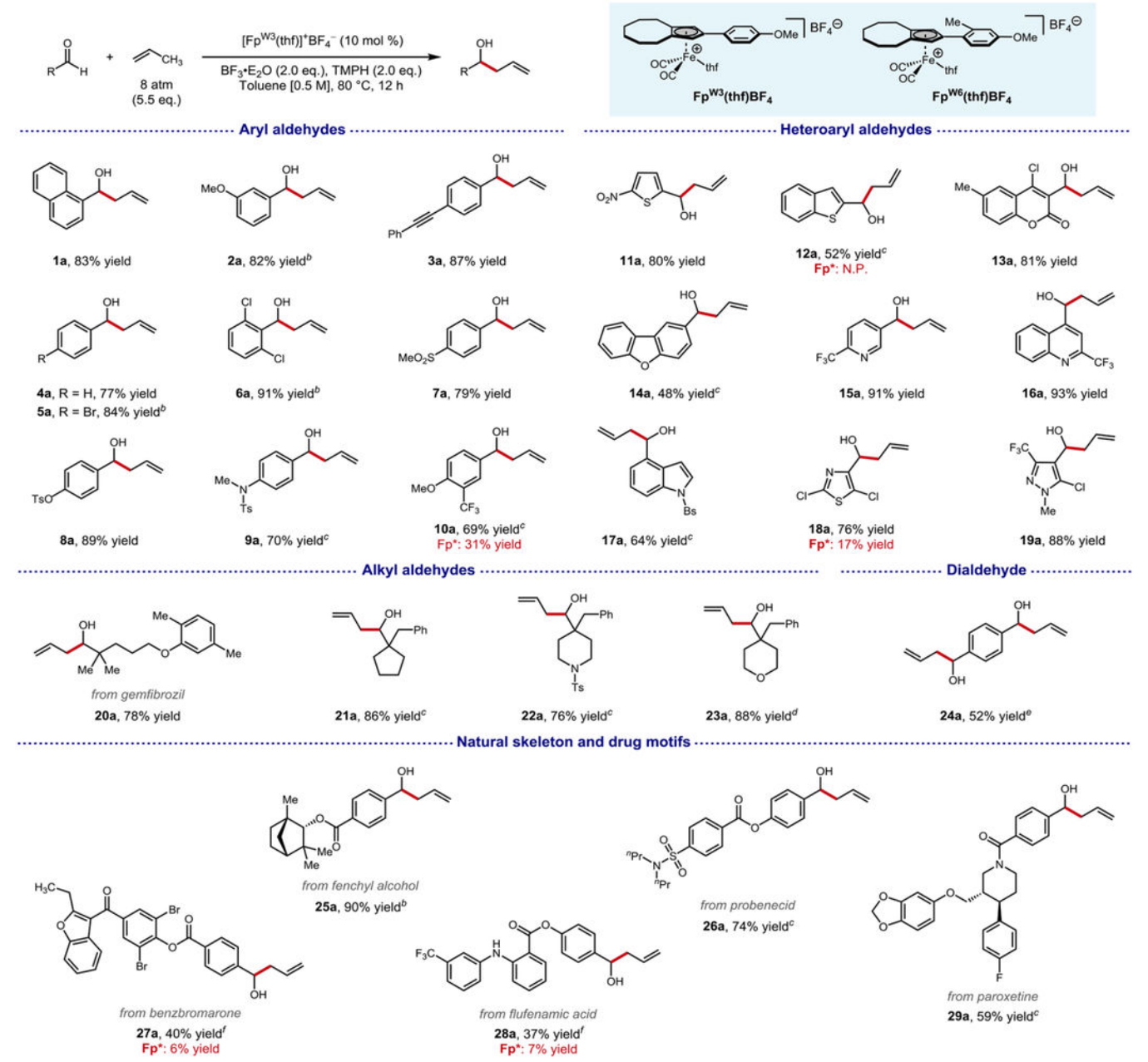

[a] Conditions: aldehyde (0.2 mmol), propylene (8 atm initial pressure, 5.5 eq.), $[Fp^{W3}(thf)]^+BF_4^-$ (10 mol %), $BF_3{\bullet}Et_2O$ (2.0 eq.), TMPH (2.0 eq.), toluene (0.4 mL), 80 °C, 12 h.

[b] 5 mol % $[Fp^{W3}(thf)]^+BF_4^-$.

[c] TMPH (3.0 eq.), $Zn(NTf_2)_2$ (10 mol %) was added.

[d] $BF_3{\bullet}Et_2O$ (3.0 eq.), TMPH (3.0 eq.).

[e] 0.1 mmol scale, $[Fp^{W3}(thf)]^+BF_4^-$ (20 mol %), $BF_3{\bullet}Et_2O$ (4.0 eq.), TMPH (6.0 eq.), $Zn(NTf_2)_2$ (20 mol %), toluene (0.2 mL).

[f] 10 mol % $[Fp^{W6}(thf)]^+BF_4^-$.

Table 2.

Scope of non-aldehyde electrophiles for the functionalization of propylene.

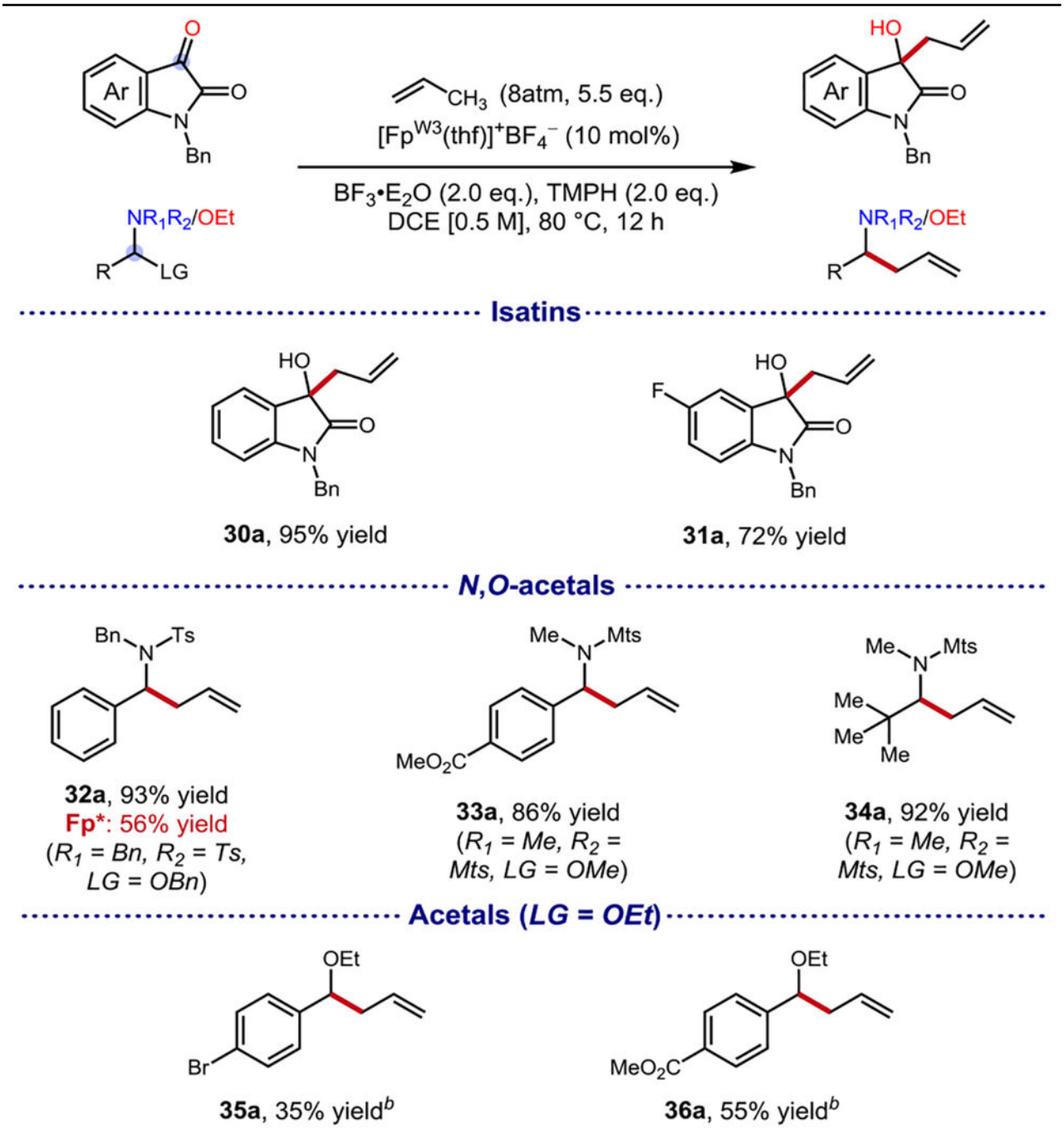

[a] Conditions: electrophile (0.2 mmol), propylene (8 atm initial pressure, 5.5 eq.), $[Fp^{W3}(thf)]^{+}BF_4^-$ (10 mol %), $BF_3{\cdot}Et_2O$ (2.0 eq.), TMPH (2.0 eq.), DCE (0.4 mL), 80 °C, 12 h.

[b] toluene (0.4 mL), 100 °C.

Angew Chem Int Ed Engl. Author manuscript; available in PMC 2024 March 01.

Table 3.

Olefin Scope for the allylic C−H functionalization of simple olefins.

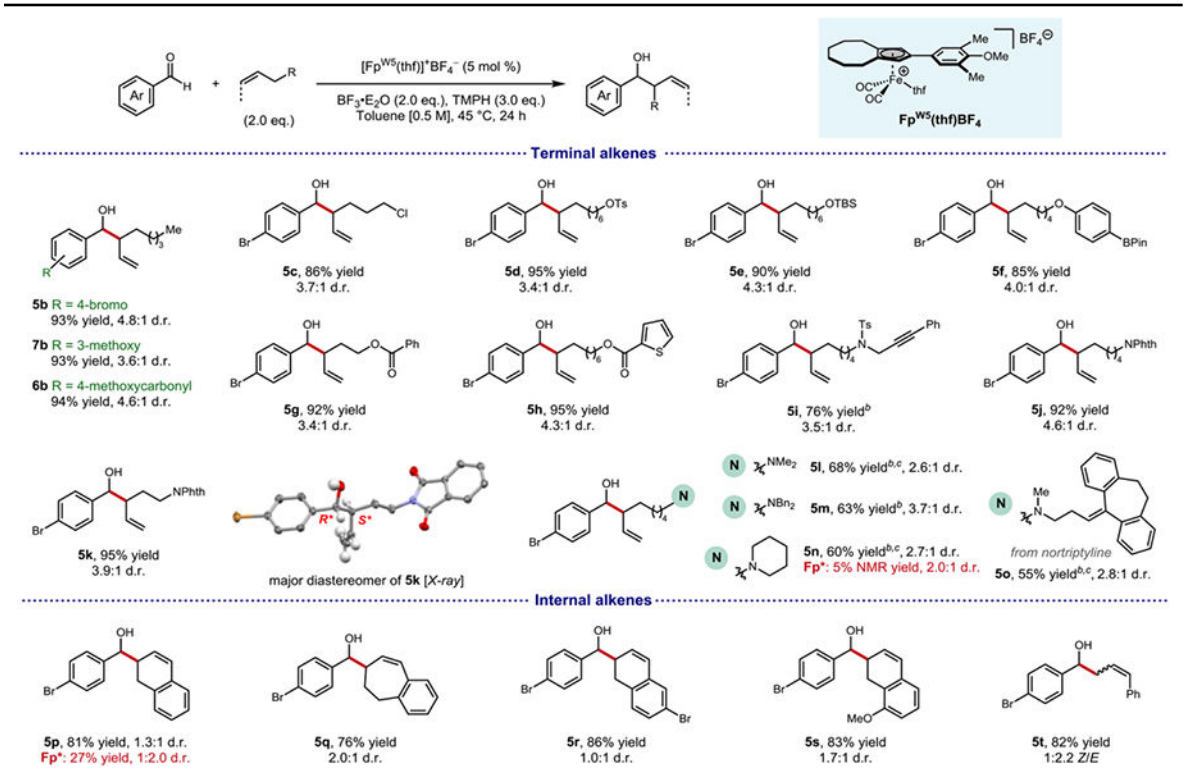

[a]Conditions: aldehyde (0.2 mmol), alkene (2.0 eq.), $[Fp^{W5}(thf)]^{+}BF_4^{-}$ (5 mol %), $BF_3{\bullet}Et_2O$ (2.0 eq.), TMPH (3.0 eq.), toluene (0.4 mL), 45 °C, 24 h.

[b]10 mol % $[Fp^{W5}(thf)]^{+}BF_4^{-}$.

[c]alkene (1.5 eq.), $BF_3{\bullet}Et_2O$ (3.0 eq.).